MOLECULAR CARCINOGENESIS 45:594–604 (2006)

Augmented Cancer Resistance and DNA Damage Response Phenotypes in PPM1D Null Mice

Bonnie Nannenga,[1] Xiongbin Lu,[2] Melissa Dumble,[2] Marc Van Maanen,[2] Thuy-Ai Nguyen,[2,3] Richard Sutton,[2] T. Rajendra Kumar,[4,5] and Lawrence A. Donehower[1,2,3]*

[1]*Department of Molecular and Cellular Biology, Baylor College of Medicine, Houston, Texas*
[2]*Department of Molecular Virology and Microbiology, Baylor College of Medicine, Houston, Texas*
[3]*Department of Interdepartmental Program in Cell and Molecular Biology, Baylor College of Medicine, Houston, Texas*
[4]*Department of Pathology, Baylor College of Medicine, Houston, Texas*
[5]*Department of Molecular and Integrative Physiology, The University of Kansas Medical Center, Kansas City, Kansas*

The p53-induced serine/threonine phosphatase, protein phosphatase 1D magnesium-dependent, delta isoform (PPM1D) (or wild-type p53-induced phosphatase 1 (Wip1)), exhibits oncogenic activity in vitro and in vivo. It behaves as an oncogene in rodent fibroblast transformation assays and is amplified and overexpressed in several human tumor types. It may contribute to oncogenesis through functional inactivation of p53. Here, we show that the oncogenic function of PPM1D is associated with its phosphatase activity. While overexpressed PPM1D may be oncogenic, *PPM1D* null mice are resistant to spontaneous tumors over their entire lifespan. This cancer resistance may be based in part on an augmented stress response following DNA damage. *PPM1D* null mice treated with ionizing radiation display increased p53 protein levels and increased phosphorylation of p38 MAP kinase, p53, checkpoint kinase 1 (Chk1), and checkpoint kinase 2 (Chk2) in their tissues compared to their wild-type (WT) counterparts. Male *PPM1D* null mice show a modest reduction in longevity, reduced serum insulin-like growth factor 1 (IGF-1) levels, and reduced body weight compared to WT mice. The *PPM1D* null mouse phenotypes indicate that PPM1D has a homeostatic role in abrogating the DNA damage response and may regulate aspects of male longevity.

Key words: p53; Chk1; Chk2; Wip1; p38 MAP kinase

INTRODUCTION

The tumor suppressor p53 is a critical stress response protein that maintains genomic integrity in part through its transcriptional regulation of a large array of genes that modulate cell growth and death pathways [1]. While most of the genes transactivated by p53 are antiproliferative in nature, there are exceptions. For example, p53 upregulates transcriptional expression of murine double minute 2 (MDM2), an E3 ubiquitin ligase that facilitates degradation of p53 in a negative feedback regulatory loop [2,3]. Thus, p53 may initiate its own destruction when it has completed its antiproliferative functions, allowing time for DNA repair before the cell reverts to a normal prestress state. Dysregulation of MDM2 expression can have deleterious effects, however, as MDM2 amplification or constitutive overexpression is observed in some human tumors [4]. Most tumors with amplified MDM2 retain wild-type (WT) p53, suggesting that the primary oncogenic role of MDM2 is to inactivate p53 function through its accelerated destruction [4].

A similar homeostatic role may be played by the p53-induced phosphatase, protein phosphatase 1D magnesium-dependent, delta isoform (PPM1D) (or wild-type p53-induced phosphatase (Wip1)). PPM1D is a type 2C serine/threonine phosphatase that is transcriptionally upregulated in a p53-dependent manner following treatment of cells with a number of stresses, including DNA damage induced by ultraviolet or ionizing radiation [5,6]. The increased PPM1D levels affect multiple stress response pathways in the cell. For example, PPM1D dephosphorylates p38 MAP kinase on threonine 180, reducing the kinase activity of p38 [6]. Because p38 phosphorylates p53 and facilitates its activation, high PPM1D levels may inhibit p53 function through p38 inactivation. In addition, PPM1D may suppress $p16^{INK4A}$ and $p19^{ARF}$ tumor suppressor activities [7]. Finally, we and others have shown that PPM1D dephosphorylates p53, checkpoint kinase 1 (Chk1), and checkpoint kinase 2 (Chk2), key cell cycle checkpoint effectors, and DNA damage

Abbreviations: MDM2, murine double minute 2; WT, wild-type; PPM1D, protein phosphatase 1D magnesium-dependent, delta isoform; Chk1, checkpoint kinase 1; Chk2, checkpoint kinase 2; PP2C, protein phosphatase, type 2C; UNG2, nuclear isoform of uracil DNA glycosylase; REFs, rat embryo fibroblasts; MEFs, mouse embryo fibroblasts; IGF-1, insulin-like growth factor 1; ATM, ataxia-telangiectasia mutated; ATR, ataxia-telangiectasis and Rad3-related.

*Correspondence to: Department of Molecular Virology and Microbiology, Baylor College of Medicine, One Baylor Plaza, Houston, TX 77030.

Received 19 September 2005; Revised 4 January 2006; Accepted 4 January 2006

DOI 10.1002/mc.20195

response proteins [8,9]. PPM1D was shown to directly dephosphorylate phosphoserine 15 on p53, thus providing a direct means for downregulating p53 activity. Moreover, dephosphorylation of phosphoserine 345 on Chk1 and phosphothreonine 68 on Chk2 by PPM1D reduced kinase activity and, in the case of Chk1, was associated with abrogation of intra-S and G_2/M cell cycle checkpoints [8,9].

Downregulation of p53 and stress response kinases such as p38, Chk1, and Chk2 implicate PPM1D as a potential oncogene. In fact, PPM1D acts as an oncogene when introduced into primary rodent fibroblasts along with activated Ras [10]. Moreover, frequent amplification and overexpression of PPM1D has been found in several human tumor types, including breast cancers, neuroblastomas, ovarian clear cell adenocarcinomas, and medulloblastomas [10–14]. Interestingly, those breast cancers with amplified PPM1D generally retain WT p53, indicating that PPM1D promotes oncogenesis at least in part through its inhibition of p53 [10].

To further examine the role of PPM1D in an in vivo context, our laboratory generated a *PPM1D* knockout mouse [15]. Mice without PPM1D are viable, but exhibit several interesting phenotypes, including sporadic male runting, increased male reproductive organ atrophy, reduced male fertility, and reduced male and female immune function [15]. It was demonstrated that when mammary tumor susceptible mouse mammary tumor virus (MMTV)-c-neu and MMTV-v-Ha-ras transgenic mice were made null for *PPM1D*, there was a considerable delay in mammary tumor formation compared to their PPM1D WT transgenic counterparts [7]. It was also shown that cells from *PPM1D* null mice have augmented $p16^{INK4A}$ activity [7]. Thus, while overexpressed PPM1D may promote oncogenesis, the absence of PPM1D may promote cancer resistance. This effect is probably due at least in part to augmented p53 and $p16^{INK4A}$ activities in the normal tissues of the *PPM1D* null mice.

In this article, the phenotypes of *PPM1D* null mice are further examined with respect to spontaneous cancer incidence, longevity, and stress responses. We confirm that the absence of PPM1D confers global resistance to spontaneous cancers and that the phosphatase activity of PPM1D is probably critical for its oncogenic properties. The cancer resistance phenotypes appear to be associated with increased p53, p38, Chk1, and Chk2 activities. Thus, PPM1D affects cancer formation through modulation of multiple stress response and growth regulatory pathways.

MATERIALS AND METHODS

PPM1D Plasmids

The mouse *PPM1D* gene was cloned by reverse transcriptase (RT)-polymerase chain reaction (PCR) from total RNA isolated from heart tissue. Additionally, site-directed mutagenesis and targeted deletion mutations were created using PCR. Mouse *PPM1D* cDNA was generated with the following primers: 5′-CCG GAT CCA TGG CGG GGC TGT ACT CGC TG-3′; 5′-GTC TGC AGT CCC AGG CCC ATC TGC GCA CAC A-3′ and SuperScript II RT (Life Technologies #18064-014). PCR products were cloned into pDrive Vector according to the manufacturer's protocol (Qiagen #231122). Mouse *PPM1D* cDNA was subcloned into pcDNA4/V5-His (Invitrogen #V861-20) at *Bam*HI and *Eco*RV. Truncation mutants were generated by PCR using pDCV-mPPM1D as template. Truncation primers: ΔN(1-49)-mPPM1D (5′-ATG CCG GCG ACC CCC ACT CTC-3′/5′-TCA TTC GAA GCA CAC ACA CAC TGT TTT CCG GTG-3′); ΔN(1-101)-mPPM1D (5′-ATG GGT CGG GAG GCG GCA CAG-3′/5′-TCA TTC GAA GCA CAC ACA CAC TGT TTT CCG GTG-3′); ΔC(376-598)-mPPM1D (5′-TCC GGA TCC ATG GCG GGG-3′/5′-TCA TTC GAA AGG GCT ATC AGT CAG GTT CAG AAA GA-3′). Truncation constructs were subcloned into pcDNA4/V5-His at *Bam*HI and *Sfi*I sites. Point mutants were generated using QuikChange Site-Directed Mutagenesis Kit (Stratagene #200518) with pcDNA4-mPPM1D as template. Point mutant primers: pcDNA4-A95D (5′-CGC CGC TCT TCG GTG GCC TTC TTT GAT GTG TGC GAC GG-3′/5′-G CCC GTC GCA CAC ATC AAA GAA GGC CAC CGA AGA GCG G-3′); pcDNA4-R266A (5′-G ATT CCT TTT CTG GCT GTA GCA AGG GCG CTT GGT GAC TTG TGG AG-3′/5′-CT CCA CAA GTC ACC AAG CGC CCT TGC TAC AGC CAG AAA AGG AAT C-3′); pcDNA4-D307A (5′-G TAT ATT ATC CTG GGA AGT GCT GGA CTT TGG AAT ATG GTT CCA CC-3′/5′-GG TGG AAC CAT ATT CCA AAG TCC AGC ACT TCC CAG GAT AAT ATA C-3′). All clones were sequenced to verify correct mutations.

In Vitro Phosphatase Assays

In vitro phosphatase reactions were carried out as described previously [16]. Briefly, reactions were performed in protein phosphatase, type 2C (PP2C) Reaction Buffer (1× PP2C Buffer, BSA at 1 mg/mL), with or without 30 mM $MgCl_2$. Enzymatic reactions were carried out at 25°C for 20 min in a Thermomixer (Eppendorf) upon addition of purified PPM1D (50 ng). Free phosphate was determined by the malachite green/molybdate-based assay, Serine/Threonine Phosphatase Assay System (Promega), performed per manufacturer's instructions with a few modifications. Phosphopeptides of interest were used in place of the supplied Ser/Thr peptide. Absorbance was measured with a 630-nm filter in a 96-well plate reader (Victor2 1400 Multilabel Plate Reader, Perkin Elmer). The amount of free phosphate was calculated by a KH_2PO_4 phosphate standard curve. These results were quantitated based on enzyme input determined by Western blot and

subsequent densitometry for immunoprecipitated protein. The phosphopeptide sequences used as substrates in these experiments were obtained from UpState Biotechnologies (p38) or New England Peptide (nuclear isoform of uracil DNA glycosylase (UNG2)); p38(180pT182pY): Ac-T-D-D-E-M-(pT)-G-(pY)-V-A-T-C-amide (positive control); UNG2 (31pT): Ac-A-V-Q-G-(pT)-G-V-A-G-V-amide (negative control).

Generation of Retroviral Vectors

The cDNAs for wt PPM1D and PPM1D.D307A were excised from the pcDNA4 plasmids described above by *Bam*HI/*Pme*I digest (thus retaining the carboxy terminus HIS-V5 tag), and subcloned into the *Bam*HI/*Sna*BI site of pBabe-Blasti. This vector encodes the blasticidin deaminase gene under the control of the SV40 promoter to allow for antibiotic selection of transduced cells. The pBabe-Ras-puro and pBabe-E1A-hygro plasmids were provided by Laura Attardi. Viral supernatants were prepared by co-transfection of 293T cells with a vesicular stomatitis virus G protein expression plasmid (pME-VSV-G) and gag-pol packaging vector (pHIT-60), and one of the retroviral vectors. After 72 h, viral supernatants were clarified by centrifugation at 3000*g* for 5 min and polybrene was added to a final concentration of 10 μg/mL. Supernatants were then frozen in aliquots at −80°C until use.

Soft Agar Assay

Rat embryonic fibroblasts (REFs) were transduced at a multiplicity of infection (MOI) of 0.1 with VSV-G-pseudotyped pBabe-E1A-hygro, and transduced cells were selected in the presence of 0.4 mg/mL hygromycin B. These E1A-expressing REFs (REF.E1A) were then super-transduced at low MOI with either control (empty vector), Ras, wt PPM1D or D307A-PPM1D mutant, and transduced cells were then selected by exposure to 10 μg/mL of puromycin (Ras vector) or 10 μg/mL of blasticidin (control, wt PPM1D and D307A-PPM1D vectors). These double integrants were used for the soft agar assay. A 0.6% noble agar/DMEM plus 10% FBS underlay was poured into 60-mm dishes. Following this, 10^5 cells were filtered and added to 3 mL of 0.4% noble agar/DMEM supplemented with 10% FBS. The mixture was layered on top of the underlay. The assay was maintained at 37°C/5% CO_2 for 12 d, being fed with 1.5 mL of 0.4% noble agar/DMEM+10% FBS every 3 d. Colonies were visualized under phase contrast at 10× magnification.

Focus Formation Assay

REF.E1A cells (produced as described above) were plated onto 10-cm plates at approximately 50% confluency. The following day, REF.E1A cells were transduced with either 1 mL of control, wt PPM1D or D307A PPM1D retrovirus, or 100 μL of the Ras-encoding retrovirus. The transduced cells were cultured for 9 d, and were fed every 3 d. On the ninth day the cultures were fixed in methanol for 20 min and stained for 2 h with Giemsa stain and transformation foci were counted.

Mice

PPM1D+/+, *PPM1D*+/−, and *PPM1D*−/− mice were bred and monitored in the Baylor College of Medicine vivarium. The *PPM1D* mice were of mixed C57BL/6 X 129/Sv background, but all mice were backcrossed at least three generations into C57BL/6. All three *PPM1D* genotypes were generated in each litter by crossing *PPM1D*+/− parents. Experiments comparing *PPM1D*−/− and *PPM1D*+/+ cells, mice, and tissues were performed using littermate samples. Only virgin males and females were used for this study. Mice were allowed to age naturally and monitored for tumor formation throughout their lifetime. All spontaneous tumors identified were harvested and fixed in 10% neutral buffered formalin. Severely moribund mice were sacrificed and all major organs analyzed by visual examination and histopathology. Histopathology of neoplastic growths was performed on hematoxylin and eosin stained sections to confirm and identify tumor type. Longevity curves were generated using StatView 5.0 to construct Kaplan–Meier plots.

Western Blot Analyses

PPM1D+/+ and *PPM1D*−/− littermate male mice were treated with 5 Gy of ionizing radiation. Six hours after radiation, various tissues were harvested from each mouse and homogenized, lysed in Tris-saline buffer pH 7.4 (50 mM Tris buffer and 120 mM NaCl) containing 1% SDS and protease inhibitors (Roche, Cat# 10946700). Lysates (20 μg) from each sample were mixed with the same volume of 2× Laemmli sample buffer, boiled and loaded on 4–20% polyacrylamide gels. The proteins were transferred to PVDF membrane and detected using the primary antibody to the protein phosphorylation site indicated in the figure and appropriate secondary antibody. Anti-Chk1(p345S) (cat#2341), anti-p53(p15S) (cat#9284), anti-Chk1(p68T) (cat#2661), and anti-p38(p180T) (cat#9216) were purchased from Cell Signaling, and anti-Actin antibody (cat#1616) was purchased from Santa Cruz. Anti-p38 protein antibody was purchased from Upstate (cat#05-454). p53 protein was detected by a cocktail of p53 antibodies (Santa Cruz cat#sc-100, sc-099 and Calbiochem cat# OP43, OP33, and OP09-2).

Radioimmunoassay (RIA) for IGF-I

Blood draws were collected by cardiac puncture from mice at various time points ($N=4$ for each genotype) and serum isolated. IGF-I assays were performed at Baylor College of Medicine as described previously [17]. IGF-I RIA was performed using the

manufacturer's protocol (Diagnostic Systems Laboratories, Inc. DSL-2900).

RESULTS

The Phosphatase Activity of PPM1D Is Essential for Its Oncogenicity

PPM1D is a type 2C serine/threonine phosphatase that is implicated as a human oncogene as a result of its amplification and overexpression in several human tumor types [10–14,18]. Moreover, in cell-based assays, PPM1D can collaborate with Ras and other oncogenes to transform rodent primary fibroblasts [10]. The mechanism by which PPM1D induces transformation remains unclear, though it appears probably that suppression of p53 and $p16^{INK4A}$ activities play a major role in its transforming functions. To provide further insights into the mechanisms of PPM1D oncogenicity, we made a series of truncation and point mutations in the *PPM1D* gene (Figure 1A). The *PPM1D* point mutations were made in codons likely to be in the phosphatase catalytic site. This was based on a high degree of *PPM1D* sequence conservation with the closely related PP2C alpha, a protein whose crystal structure and phosphatase catalytic sites have been determined [19]. Mutations at these sites in PP2C alpha produced a phosphatase-dead protein. Thus, the three point mutants in *PPM1D* generated at identical sites were probably phosphatase-dead mutants. Two N-terminal truncation mutants (ΔN1-49 and Δ1-101) and a C-terminal truncation mutant (ΔC376-598) were also generated. The N-terminal mutant ΔN1-101 extends into the

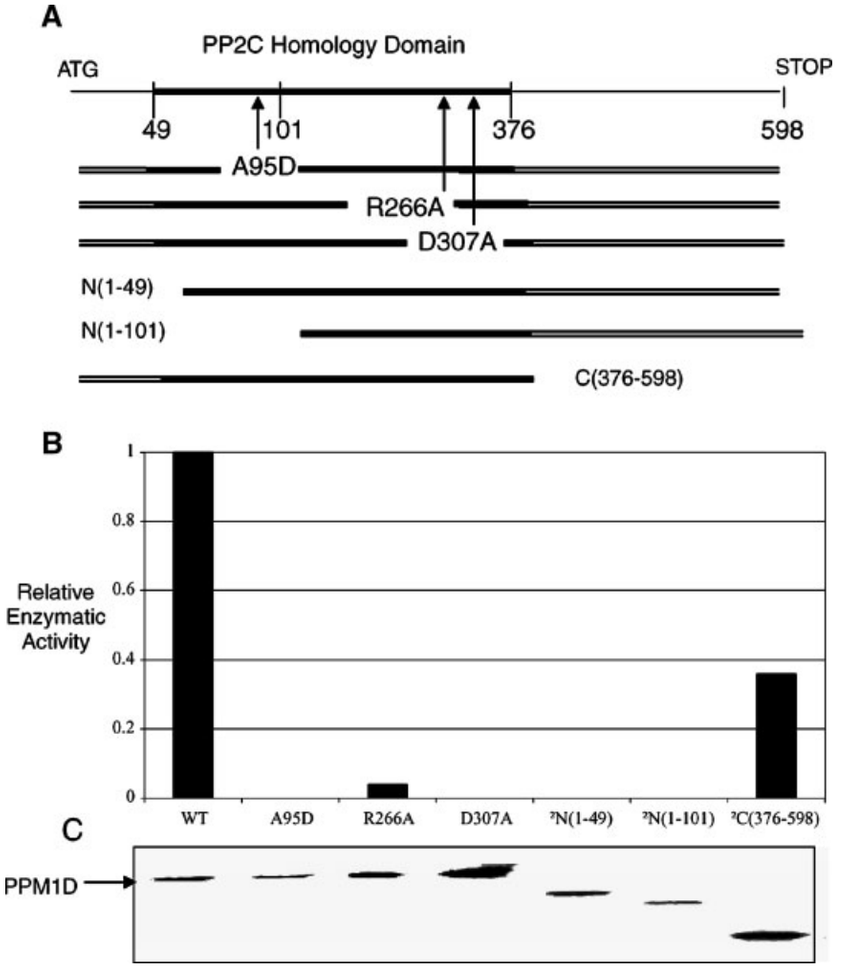

Figure 1. In vitro phosphatase activity of WT *PPM1D* and *PPM1D* mutants. (A) Schematic of the WT mouse *PPM1D* gene indicating the conserved PP2C homology region (bold line) and the mutants of mouse *PPM1D* that were generated. (B) In vitro phosphatase activity, using known PPM1D target phosphopeptide p38(180pT182pY), as a target for immunopurified V5-PPM1D obtained from *PPM1D* expression constructs, including WT, point mutants (A95D, R266A, D307A), N-terminal truncations ΔN(1-49) and ΔN(1-101), and a C-terminal truncation mutant ΔC(376-598). (C) Expression levels of WT and mutant PPM1D. CV-1 cells were transfected with the various constructs and immunoprecipitated with anti-V5. Western blot analysis was used to quantitate protein input into the phosphatase assay.

conserved phosphatase domain of PPM1D (codons 65–375), while N-terminal ΔN1-49 and the C-terminal mutant does not [5,20].

Wild-type and mutant PPM1D proteins were generated, immunopurified, and incubated with a substrate phosphopeptide derived from p38 MAP kinase. This phosphopeptide contains phosphorylated threonine 180 and tyrosine 182 that is targeted by MAP kinases in the stress response [21]. PPM1D has been shown to efficiently dephosphorylate MAP kinase threonine 180 in vivo and in vitro [6]. As a negative control phosphopeptide, we used a phosphothreonine 31 derived from uracil DNA glycosylase (UNG2) that we previously showed is not dephosphorylated by PPM1D [16]. In vitro phosphatase reactions were carried out in the presence of molybdate dye and release of free phosphate from the phosphopeptide was measured by absorbance at 630 nm. Control reactions were also performed in the absence of peptide or in the absence of magnesium (data not shown). WT PPM1D, as expected, showed high levels of in vitro phosphatase activity (Figure 1B). The C-terminal truncated mutant (ΔC376-598) exhibited some activity (about 40% of WT activity), while the N-terminal mutants (ΔN1-49 and ΔN1-101) and the three catalytic site point mutants showed little or no phosphatase activity in these reactions (Figure 1B). WT and mutant PPM1D proteins were produced at similar levels in transfected cells (Figure 1C).

It has been shown that PPM1D can collaborate with other oncogenes such as Ras to transform primary rodent fibroblasts [10]. These experiments indicate that PPM1D is an oncogene, though the mechanism of transformation by PPM1D remains unclear. To determine whether the phosphatase activity of PPM1D is essential or dispensable for its oncogenic activity, we performed two types of transformation assays with WT PPM1D and a phosphatase-dead mutant of PPM1D. We generated two retroviral vector constructs, one expressing WT PPM1D and the other phosphatase-dead PPM1D mutant D307A. The D307A mutant has previously been shown to be defective for in vitro and in vivo dephosphorylation of p53 at serine 15 and Chk1 at serine 345, while the WT PPM1D efficiently dephosphorylates these sites [8]. However, the phosphatase-dead D307A mutant does bind as efficiently to PPM1D targets UNG2 and Chk1 as the WT protein [8,16].

Wild-type PPM1D, phosphatase-dead PPM1D, mutant Ras, and empty retroviral vectors were transduced into REFs previously transduced with an E1A-expressing retroviral vector (REF.E1A cells). Nine days following vector transduction the REFs displayed obvious transformation foci and these were counted. Two separate experiments showed that WT PPM1D formed foci in the presence of E1A, but not nearly as many as that formed by mutant Ras (Figure 2A and B). When normalized to infectious units of retrovirus transduced, about 30% of Ras retroviruses formed foci, while about 0.3% of WT PPM1D retroviruses formed foci. Thus, PPM1D is not as potent an oncogene as mutant Ras, but it is clearly oncogenic, as control retrovirus produced no detectable foci in the assay (Figure 2A and B). Interestingly, the D307A phosphatase-dead mutant PPM1D also produced no foci, suggesting that the phosphatase activity of PPM1D is absolutely required for its oncogenic activity.

To confirm that PPM1D could also confer anchorage independence, another marker of transformation, we performed a soft agar assay on the REF.E1A cells. Both Ras- and WT PPM1D-expressing vectors transduced into E1A REFs resulted in numerous colonies of cells growing in soft agar, while control vector and phosphatase-dead PPM1D vector transduction did not result in soft agar colony formation (Figure 2C and D). The absence of foci and growth in soft agar resulting from transduction of the phosphatase-dead PPM1D mutant was not a result of inadequate PPM1D protein expression, as REF.E1A cells transduced with both WT and phosphatase-dead PPM1D showed equivalent high levels of PPM1D protein expression as measured by Western blot analysis (Figure 2E).

The PPM1D Null Mouse Is Resistant to Spontaneous Tumors

Overexpression of PPM1D appears to be oncogenic, both in vitro in fibroblast transformation assays and in vivo as a result of amplification and overexpression of PPM1D in a subset of human tumors. Conversely, it has been shown that *PPM1D* null mouse embryo fibroblasts (MEFs) are resistant to transformation by oncogenes and that some mammary tumor susceptible transgenic mice are resistant to mammary tumors in the absence of PPM1D [7]. To test this further, we monitored genetic background matched cohorts of *PPM1D*+/+, *PPM1D*+/−, and *PPM1D*−/− mice over their lifespan for cancer incidence. Morbid or dead mice were necropsied and tissues assessed by histopathological analysis for tumors. We found that the three *PPM1D* genotypes showed a correlation between tumor incidence and PPM1D dosage (Figure 3). The *PPM1D*+/+ mice displayed a 45% incidence of cancers, mostly lymphomas. This spectrum and incidence rate of tumors was consistent with our previous analyses on WT mice of this strain (predominantly C57BL/6) [22]. A quarter of the *PPM1D*+/− mice succumbed to cancer, while only 10% of the *PPM1D* null mice developed cancers (Figure 3). Tumor incidence differences between the *PPM1D*+/+ and *PPM1D*−/− mice were significant ($P = 0.016$). Thus, consistent with previous results, it appears that the absence of PPM1D confers a significant cancer resistance effect over the lifespan of the mouse.

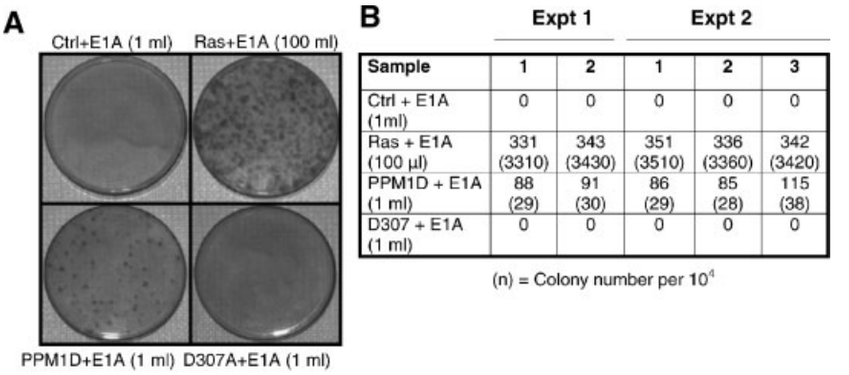

B

Sample	Expt 1		Expt 2		
	1	2	1	2	3
Ctrl + E1A (1ml)	0	0	0	0	0
Ras + E1A (100 µl)	331 (3310)	343 (3430)	351 (3510)	336 (3360)	342 (3420)
PPM1D + E1A (1 ml)	88 (29)	91 (30)	86 (29)	85 (28)	115 (38)
D307 + E1A (1 ml)	0	0	0	0	0

(n) = Colony number per 10^4

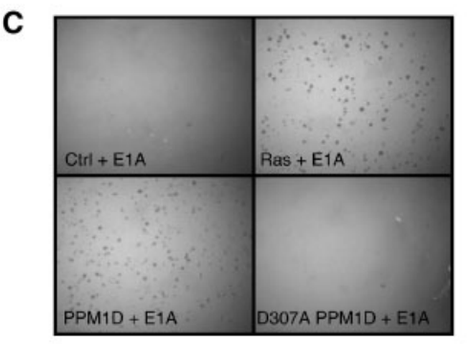

D

Sample	# Colonies
Ctrl + E1A	0
Ras + E1A	++++
PPM1D + E1A	++++
D307A + E1A	0

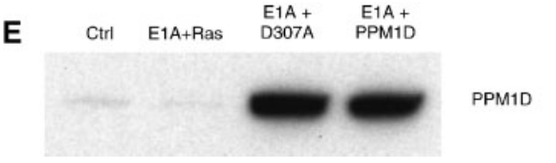

Figure 2. In vitro transformation by WT *PPM1D* and a phosphatase-dead *PPM1D* mutant (D307A). (A) Representative focus formation assay 9 d following infection of REF.E1A cells with either control, *Ras*, *PPM1D* or D307A *PPM1D* viral vectors. In parentheses is indicated the volume of virus applied. (B) Transformed focus formation when REF.E1A cells were infected with virus-expressing control, Ras, WT PPM1D or D307A phosphatase-dead PPM1D. Numbers in parentheses are corrected for virus titer and expressed as colony number per 10^4 infectious units. (C) Representative soft agar assays showing colony formation by control virus, Ras-expressing virus, WT PPM1D-expressing virus, and phosphatase-dead PPM1D-expressing virus (D307A). (D) WT but not mutant PPM1D induces anchorage-independent growth in the soft agar assay. The colony numbers of the Ras + E1A and PPM1D + E1A were comparable but were too many to count (>1500). (E) WT and mutant PPM1D proteins are expressed in similar quantities in REF.E1A cells. Western blot analysis was performed with an anti-V5 primary antibody to determine the expression of PPM1D and mutant PPM1D (V5 tagged) in the REF.E1A cells used for the transformation assays.

Increased p38, p53, Chk1, and Chk2 Phosphorylation in *PPM1D* Null Tissues

PPM1D regulates multiple DNA damage response pathways in the cell through dephosphorylation. Initially, it was shown to dephosphorylate p38 MAP kinase on phosphothreonine 180 and reduce p38 activity [6]. Subsequently, our laboratory has shown that PPM1D dephosphorylates targets of the DNA damage response kinases ATM and ATR. These include p53 phosphoserine 15 and Chk1 phosphoserine 345 [8]. Recently, Fujimoto et al. [9] have also demonstrated that PPM1D dephosphorylates Chk2 at threonine 68. In the cases of Chk1 and Chk2, dephosphorylation by PPM1D results in decreased kinase activity [8,9]. These PPM1D dephosphorylation events are also accompanied by abrogated cell cycle checkpoints and reduced DNA repair functions [8,16]. To test whether absence of PPM1D results in an enhanced DNA damage response in vivo, we irradiated *PPM1D*+/+ and *PPM1D*−/− mice with 5 Gy ionizing radiation and analyzed tissues harvested 6 h after irradiation for phosphorylation status of known PPM1D dephosphorylation targets. Lysates from a variety of tissues were assessed by Western blot analysis with antibodies to p53 and p38 as well as phospho-specific antibodies for Chk1 phosphoserine 345, Chk2 phosphothreonine 68, p53

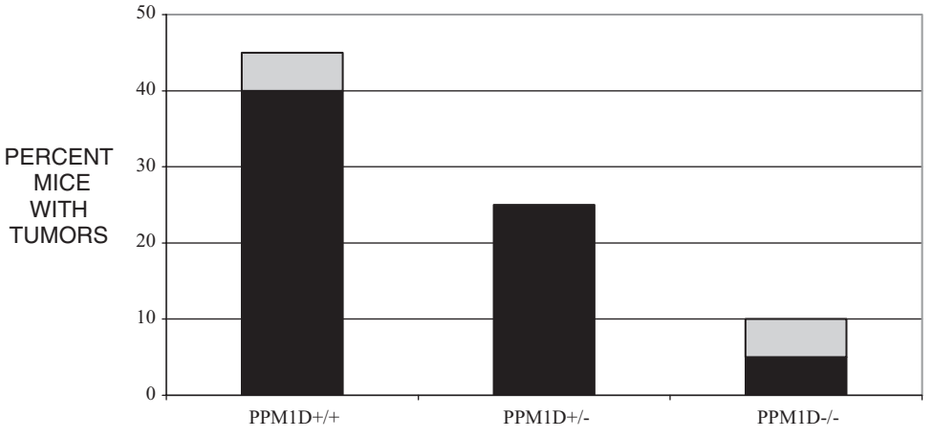

Figure 3. Lifespan tumor incidence in *PPM1D*+/+, *PPM1D*+/−, and *PPM1D*−/− mice. Twenty each of *PPM1D*+/+, *PPM1D*+/−, and *PPM1D*−/− mice were monitored over their lifetimes for spontaneous tumors. Moribund mice or dead mice were subjected to necropsy and their tissues examined by gross pathology and histopathology of major organs. Mice with and without discernable malignancies were scored for each genotype and the results are shown as percentage of each *PPM1D* genotype that developed tumors. The black portion of each bar represent lymphomas, while gray portions represent nonlymphoid tumors (sarcomas).

phosphoserine 15, and p38 phosphothreonine 180. Lysates from unirradiated tissues showed little phosphorylation regardless of *PPM1D* genotype (data not shown), but lysates from irradiated tissues showed variable phosphorylation patterns. In many tissues, there was no PPM1D-dependent difference between protein phosphorylation levels of the various proteins (Figure 4). However, a sizeable number of tissues did display differences in protein phosphorylation levels between *PPM1D*+/+ and *PPM1D*−/− lysates (Figure 4, asterisks). Invariably, in those tissues with differential target protein phosphorylation, PPM1D−/− tissues exhibited higher levels of protein phosphorylation, consistent with the absence of available PPM1D to dephosphorylate that target (Figure 4). The pattern of tissues that showed differential protein phosphorylation was variable with each protein analyzed. For example, Chk1 serine 345 exhibited increased phosphorylation in PPM1D−/− lung and testis, while p53 serine 15 showed increased phosphorylation in PPM1D−/− thymus, muscle, lung, and spleen. This latter pattern for p53 is similar to tissue-specific

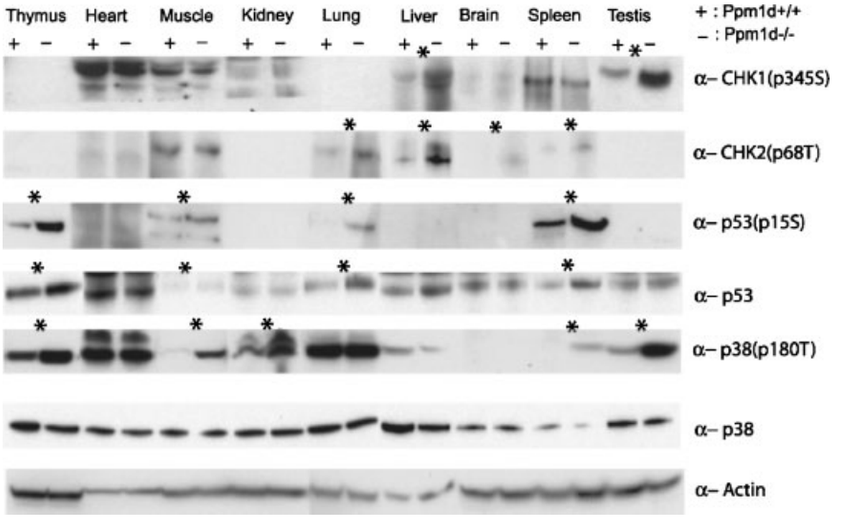

Figure 4. Protein levels and phosphorylation status of PPM1D target proteins in tissues from irradiated *PPM1D*+/+ and *PPM1D*−/− mice. *PPM1D*+/+ and *PPM1D*−/− littermate male mice were treated with 5 Gy of ionizing radiation. Six hours after radiation, various tissues were harvested from each mouse. Protein lysates from each tissue were subjected to Western blot analysis with antibodies specific for the proteins or their phosphorylated forms. Tissues with increased protein or phosphorylation levels in the *PPM1D* null mice are indicated by an asterisk.

patterns of p53 stabilization in historical irradiation studies [23]. Moreover, antibodies to p53 protein showed increased p53 protein levels in the same tissues that exhibited increased p53 serine 15 phosphorylation (Figure 4, third and fourth rows). Three of the PPM1D target proteins (Chk2, p53, and p38) showed increased phosphorylation in four PPM1D−/− tissues, while Chk1 showed increased phosphorylation in only two PPM1D−/− target tissues. Thus, stress kinase phosphorylation sites targeted by PPM1D are targeted in some intact irradiated tissues as well as in cells in tissue culture.

Longevity and Aging Phenotypes in PPM1D Null Mice

In our initial studies of *PPM1D* null mice, we reported that the *PPM1D*−/− males exhibited a moderately reduced longevity, while *PPM1D*−/− females displayed an apparent normal longevity [15]. These studies were only carried out to 2 yr of age. We have now completed a full lifespan study on another group of *PPM1D*+/+, *PPM1D*+/−, and *PPM1D*−/− mice. Monitoring of the *PPM1D*−/− males confirmed that they had a modest but significant reduction in mean longevity compared to their *PPM1D*+/+ male counterparts, as well as the *PPM1D*−/− females (Figure 5). *PPM1D*−/− males had a mean longevity of 96 wk and a maximal longevity of 122 wk, compared to a mean longevity of 128 wk and a maximal longevity of 162 wk for PPM1D+/+ males of the same genetic background. This difference was highly significant ($P < 0.0001$) (Figure 5A). Similarly, the *PPM1D*−/− males had significant reductions in mean and maximal longevity in comparison to *PPM1D*−/− females ($P = 0.009$) (Figure 5B). The *PPM1D*+/− males had similar longevity to the WT males (data not shown). *PPM1D*−/− females had mean and maximal longevities of 118 and 142 wk, respectively, compared to *PPM1D*+/+ females with mean and maximal longevities of 121 and 156 wk, respectively (Figure 5C). These null *PPM1D* lifespan measurements were not significantly different from WT *PPM1D* females.

Monitoring of the *PPM1D*−/− males indicated that they maintained a reduction in body mass over their lifespan and by 2 yr of age appeared less robust than their WT counterparts (Figure 6A and B). The *PPM1D* null males tended to exhibit more ruffled fur, lordokyphosis (hunchbacked spine) and more sluggish activity compared to their age- and sex-matched WT counterparts, though this was somewhat variable in degree. *PPM1D*−/− females did not display any of the aging phenotypes described above for the males, though they did show a slight, though not significant, reduction in body weight as they became older (Figure 6C). Histopathological analyses of various tissues from 20 to 24 mo *PPM1D*−/− and *PPM1D*+/+ male mice did not reveal any obvious differences in tissue organization or age-related

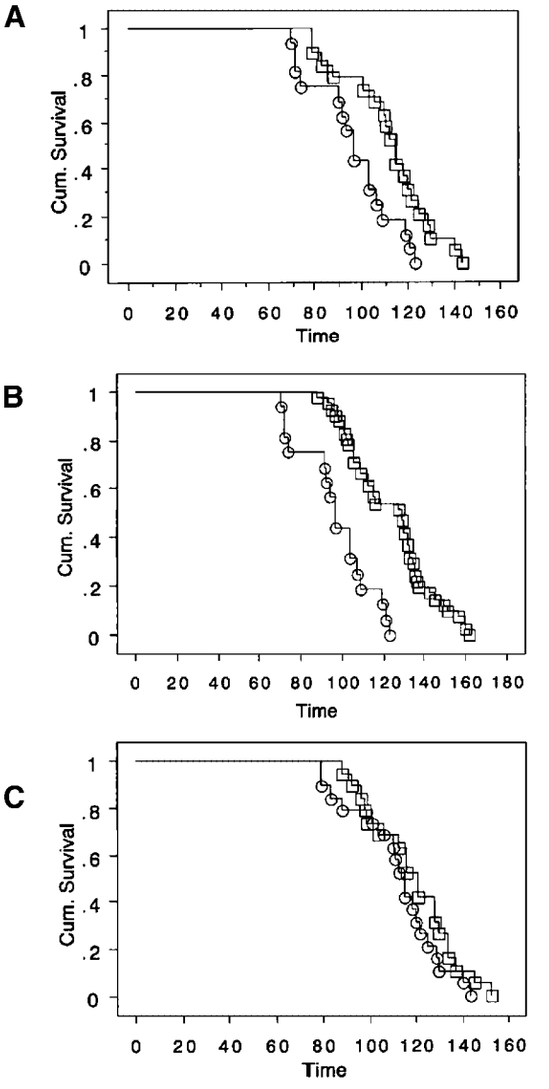

Figure 5. Longevity of *PPM1D*-deficient and WT mice. (A) Kaplan–Meier plot of *PPM1D*−/− male survival (circles) compared to *PPM1D*+/+ male survival (squares). (B) Kaplan–Meier plot of *PPM1D*−/− male survival (circles) compared to *PPM1D*−/− female survival (squares). (C) Kaplan–Meier plot of *PPM1D*−/− female survival (circles) compared to *PPM1D*+/+ female survival (squares).

anomalies. Organ weights in the *PPM1D*−/− males were marginally reduced, but when normalized for body weight, there were no significant differences in comparison to WT organs (Figure 6D). Thus, older *PPM1D*−/− males exhibited only subtle alterations in aging phenotypes compared to *PPM1D*+/+ mice, despite having a modestly reduced longevity. There was no evidence that the reduced longevity of the *PPM1D*−/− males was due to increased pathogen infections, because there were no obvious signs of increased infection or inflammation in the tissues of these mice.

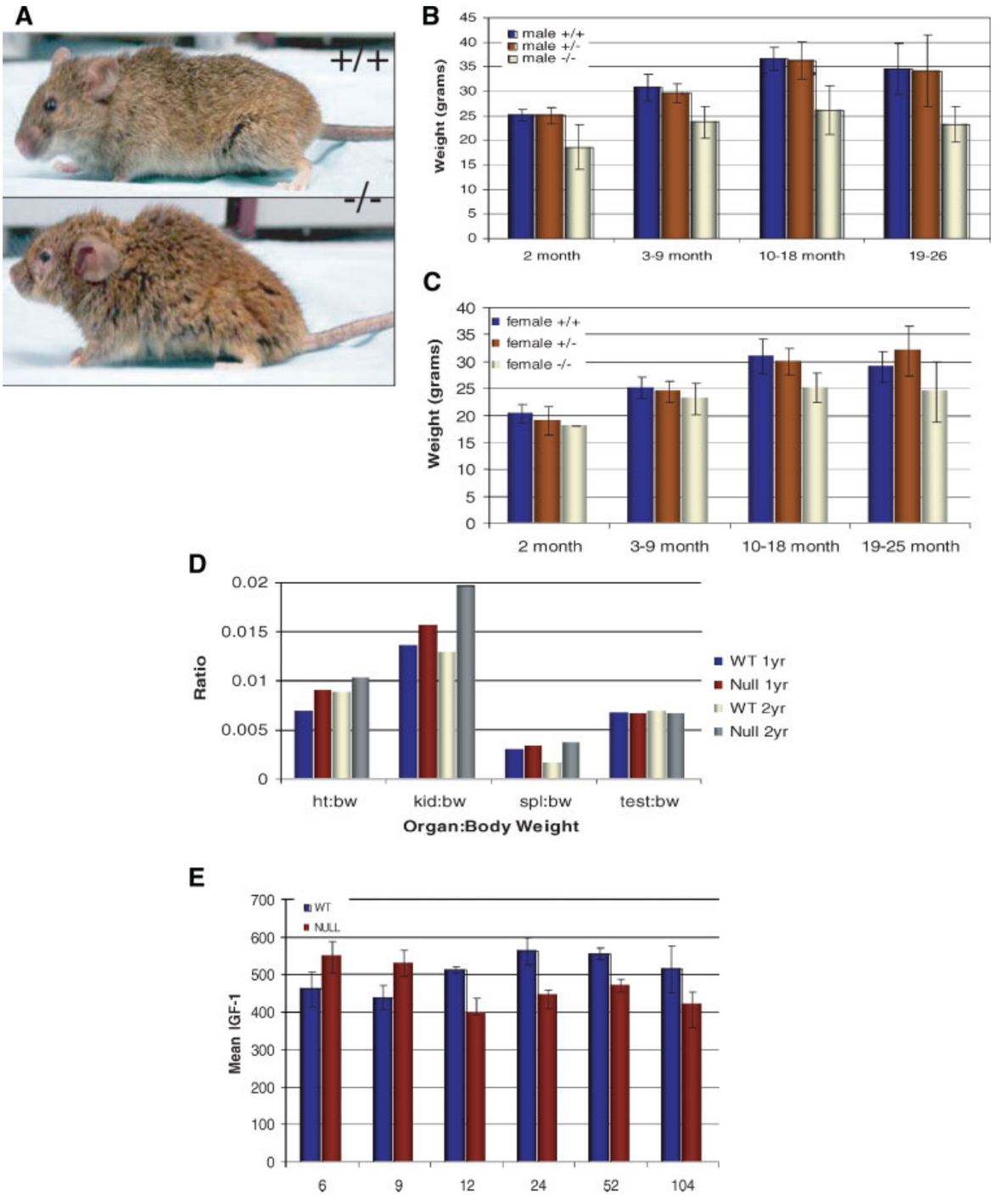

Figure 6. Aging phenotypes in *PPM1D* null and WT mice. (A) Representative 2-yr-old *PPM1D* WT (top) and null (bottom) males are shown. (B) Mean body weights of *PPM1D*+/+, *PPM1D*+/−, and *PPM1D*−/− males at different ages. (C) Mean body weights of *PPM1D*+/+, *PPM1D*+/−, and *PPM1D*−/− females at different ages. (D) Mean organ mass to body weight ratios in *PPM1D* null and *PPM1D* WT mice at 1 and 2 yr of age. (E) Mean serum IGF-1 levels in *PPM1D* null (red bars) and WT *PPM1D* (blue bars) male mice at different ages.

Alterations in longevity have been associated with altered insulin/insulin-like growth factor 1 (IGF-1) signaling in a number of model organisms [24,25]. We examined serum IGF-1 levels in the *PPM1D*+/+ and *PPM1D*−/− males at different ages up to 2 yr. At early ages (6 and 9 wk), *PPM1D*−/− males averaged moderately higher levels of serum IGF-1 than the *PPM1D*+/+ males (Figure 6E). By 24 wk and thereafter, however, IGF-1 levels were consistently lower in the PPM1D−/− males compared to their WT counterparts. Whether the reduced IGF-1 levels in the older PPM1D null males was a causal factor in their cancer resistance, reduced body weight, and less robust appearance remains unclear.

DISCUSSION

Evidence is accumulating that *PPM1D* is a significant human oncogene [18,26]. *PPM1D* is oncogenic in rodent transformation assays and is amplified and overexpressed in several human tumor types [10–13]. A major component of PPM1D oncogenicity is probably a result of its effects on p53 inactivation. Moreover, $p16^{INK4A}$ and p38 MAP kinase signaling may also be inhibited by PPM1D [6,7]. Here we show through in vitro transformation assays that the oncogenic activity of PPM1D appears to be dependent on its phosphatase activity. A full-length PPM1D with a single amino acid change rendering its catalytic phosphatase activity nonfunctional results in a protein with no in vitro transforming activity. In contrast, WT *PPM1D* in conjunction with E1A reliably transforms primary fibroblasts, though at a reduced efficiency compared to E1A plus mutant Ras. Thus, PPM1D is oncogenic through dephosphorylation of critical targets. We have previously shown that PPM1D directly dephosphorylates p53 at serine 15 and may reduce p53 serine 20 phosphorylation through suppression of Chk1 kinase activity [8,27]. PPM1D may also reduce p38 MAP kinase phosphorylation of p53 at serines 33 and 46 through dephosphorylation of p38 [6,28]. Finally, PPM1D may also suppress p53 activity through suppression of $p19^{ARF}$ [7].

While overexpression of PPM1D can be oncogenic, reduction in PPM1D dosage can be antioncogenic. *PPM1D* null fibroblasts have been shown to be resistant to oncogene transformation and *PPM1D* null mice are resistant to oncogene-induced mammary carcinogenesis [7]. Here, we show that *PPM1D* null mice are globally resistant to spontaneous tumors and even the *PPM1D* heterozygotes appear to have some reduction in tumor formation as compared to WT mice. Again, a major component of this cancer resistance is likely to be increased p53 activity in the *PPM1D* null mice. We have previously shown that *PPM1D* null MEFs have increased p53 activity as measured by serine 15 phosphorylation and $p21^{CIP1}$ induction [15]. Moreover, in other MEF studies we have demonstrated that radiation treatment of *PPM1D* null MEFs results in dramatically higher levels of p53 serine 15 phosphorylation than similarly treated WT MEFs [8]. Here, we directly examine tissues from mice treated with ionizing radiation and show that in at least four organs of the *PPM1D* null mice, p53 serine 15 phosphorylation and protein levels are higher than in the same organs of the irradiated WT mice. Interestingly, the p53 serine 15 and p38 MAP kinase threonine 180 phosphorylation response was particularly pronounced in the thymus and spleen of the irradiated *PPM1D* null mice. The tumors that arise in this strain of mice (predominantly C57BL/6) are largely lymphomas, so that augmented p53 and p38 stress responses in lymphoid organs are likely to contribute to the observed resistance of the PPM1D null mice to lymphomas.

Recently, we have reported that PPM1D dephosphorylates Chk1 at phosphoserine 345, which, like p53 phosphoserine 15, is another target of ataxia-telangiectasia mutated (ATM)/ataxia-telangiectasis and Rad3-related (ATR) phosphorylation in response to DNA damage [8]. Chk1 is an important component of the G_2/M checkpoint and we showed that overexpression of PPM1D abrogates cell cycle checkpoints. Fujimoto et al. [9] have shown that PPM1D dephosphorylates Chk2 at phosphothreonine 68 and reduces Chk2 kinase activity. Here, we show that ATM/ATR target sites Chk1 serine 345 and Chk2 threonine 68 have enhanced phosphorylation in some of the irradiated *PPM1D*−/− tissues in comparison to their WT counterparts. Thus, enhanced checkpoint responses following damage or stress in the PPM1D null organs could also contribute to the cancer resistance observed in the PPM1D-deficient mice. These enhanced DNA damage responses may be particularly relevant to cancer prevention given the recent demonstration that the ATM-Chk2-p53 DNA damage response pathways are activated in many human preneoplastic lesions [27,28].

The effects of PPM1D on reducing male longevity are of some interest. In general, aged *PPM1D*−/− males appeared less robust than their female age-matched counterparts and reasons for the sex-specific differences remain a mystery. In earlier studies we showed that *PPM1D* RNA is expressed at moderate levels in all tissues, but that it is expressed at extremely high levels in the testes [20]. Moreover, atrophy of male reproductive organs with age is pronounced in the null mice. We attempted to shed some light on this by examining hormone levels in the mice. The only significant enduring difference in the *PPM1D* WT and null mice was observed for IGF-1. IGF-1 levels remained significantly reduced in the *PPM1D* null males throughout most of their life span. This observation may partially explain the reduced body weight and lack of robustness observed in the null males, because age-related muscle atrophy, bone loss, and other parameters have been associated

with reduced growth hormone/IGF-1 levels in the blood with age [29,30]. The reduced IGF-1 levels in the *PPM1D* null males may also play a part in the reduced tumor incidence, as high IGF-1 levels have been correlated with higher cancer incidences in humans [31].

In conclusion, we have performed further functional characterization of PPM1D in both in vitro and in vivo contexts. We have shown that the phosphatase activity of PPM1D is probably essential for its transformation capability. We have also shown that *PPM1D*-deficient mice exhibit a range of interesting phenotypes, most notably an augmented stress response and a global resistance to cancer. It is clear that reducing PPM1D dosage has a powerful effect in reducing cancer susceptibility and that PPM1D could perhaps be exploited in a therapeutic modality to suppress cancer in humans.

ACKNOWLEDGMENTS

We thank Laura Attardi for providing retroviral vector constructs. We also thank Ron Javier for supplying us with rat embryo fibroblasts and reagents for the in vitro transformation assays. This work was supported by a grant from the National Cancer Institute to L.A.D. (CA100420).

REFERENCES

1. Vousden KH, Lu X. Live or let die: The cell's response to p53. Nat Rev Cancer 2002;2:594–604.
2. Meek DW. The p53 response to DNA damage. DNA Repair (Amst) 2004;3:1049–1056.
3. Moll UM, Petrenko O. The MDM2-p53 interaction. Mol Cancer Res 2003;1:1001–1008.
4. Momand J, Jung D, Wilczynski S, Niland J. The MDM2 gene amplification database. Nucleic Acids Res 1998;26:3453–3459.
5. Fiscella M, Zhang H, Fan S, et al. Wip1, a novel human protein phosphatase that is induced in response to ionizing radiation in a p53-dependent manner. Proc Natl Acad Sci USA 1997; 94:6048–6053.
6. Takekawa M, Adachi M, Nakahata A, et al. p53-inducible wip1 phosphatase mediates a negative feedback regulation of p38 MAPK-p53 signaling in response to UV radiation. EMBO J 2000;19:6517–6526.
7. Bulavin DV, Phillips C, Nannenga B, et al. Inactivation of the Wip1 phosphatase inhibits mammary tumorigenesis through p38 MAPK-mediated activation of the p16(Ink4a)-p19(Arf) pathway. Nat Genet 2004;36:343–350.
8. Lu X, Nannenga B, Donehower LA. PPM1D dephosphorylates Chk1 and p53 and abrogates cell cycle checkpoints. Genes Dev 2005;19:1162–1174.
9. Fujimoto H, Onishi N, Kato N, et al. Regulation of the antioncogenic Chk2 kinase by the oncogenic Wip1 phosphatase. Cell Death Differ 2005.
10. Bulavin DV, Demidov ON, Saito S, et al. Amplification of PPM1D in human tumors abrogates p53 tumor-suppressor activity. Nat Genet 2002;31:210–215.
11. Li J, Yang Y, Peng Y, et al. Oncogenic properties of PPM1D located within a breast cancer amplification epicenter at 17q23. Nat Genet 2002;31:133–134.
12. Saito-Ohara F, Imoto I, Inoue J, et al. PPM1D is a potential target for 17q gain in neuroblastoma. Cancer Res 2003;63: 1876–1883.
13. Hirasawa A, Saito-Ohara F, Inoue J, et al. Association of 17q21-q24 gain in ovarian clear cell adenocarcinomas with poor prognosis and identification of PPM1D and APPBP2 as likely amplification targets. Clin Cancer Res 2003;9:1995–2004.
14. Mendrzyk F, Radlwimmer B, Joos S, et al. Genomic and protein expression profiling identifies CDK6 as novel independent prognostic marker in medulloblastoma. J Clin Oncol 2005;23:8853–8862.
15. Choi J, Nannenga B, Demidov ON, et al. Mice deficient for the wild-type p53-induced phosphatase gene (Wip1) exhibit defects in reproductive organs, immune function, and cell cycle control. Mol Cell Biol 2002;22:1094–1105.
16. Lu X, Bocangel D, Nannenga B, Yamaguchi H, Appella E, Donehower LA. The p53-induced oncogenic phosphatase PPM1D interacts with uracil DNA glycosylase and suppresses base excision repair. Mol Cell 2004;15:621–634.
17. Kumar TR, Palapattu G, Wang P, et al. Transgenic models to study gonadotropin function: The role of follicle-stimulating hormone in gonadal growth and tumorigenesis. Mol Endocrinol 1999;13:851–865.
18. Harrison M, Li J, Degenhardt Y, Hoey T, Powers S. Wip1-deficient mice are resistant to common cancer genes. Trends Mol Med 2004;10:359–361.
19. Das AK, Helps NR, Cohen PT, Barford D. Crystal structure of the protein serine/threonine phosphatase 2C at 2.0 A resolution. EMBO J 1996;15:6798–6809.
20. Choi J, Appella E, Donehower LA. The structure and expression of the murine wildtype p53-induced phosphatase 1 (Wip1) gene. Genomics 2000;64:298–306.
21. Bulavin DV, Higashimoto Y, Popoff IJ, et al. Initiation of a G2/M checkpoint after ultraviolet radiation requires p38 kinase. Nature 2001;411:102–107.
22. Venkatachalam S, Tyner SD, Pickering CR, et al. Is p53 haploinsufficient for tumor suppression? Implications for the p53+/− mouse model in carcinogenicity testing. Toxicol Pathol 2001;29:147–154.
23. MacCallum DE, Hupp TR, Midgley CA, et al. The p53 response to ionising radiation in adult and developing murine tissues. Oncogene 1996;13:2575–2587.
24. Katic M, Kahn CR. The role of insulin and IGF-1 signaling in longevity. Cell Mol Life Sci 2005;62:320–343.
25. Kenyon C. The plasticity of aging: Insights from long-lived mutants. Cell 2005;120:449–460.
26. Bernards R. Wip-ing out cancer. Nat Genet 2004;36:319–320.
27. Lu X, Nguyen TA, Donehower LA. Reversal of the ATM/ATR-mediated DNA damage response by the oncogenic phosphatase PPM1D. Cell Cycle 2005;4:1060–1064.
28. Bulavin DV, Saito S, Hollander MC, et al. Phosphorylation of human p53 by p38 kinase coordinates N-terminal phosphorylation and apoptosis in response to UV radiation. EMBO J 1999;18:6845–6854.
29. Grounds MD. Reasons for the degeneration of ageing skeletal muscle: A central role for IGF-1 signalling. Biogerontology 2002;3:19–24.
30. Zofkova I. Pathophysiological and clinical importance of insulin-like growth factor-I with respect to bone metabolism. Physiol Res 2003;52:657–679.
31. Pollak MN. Insulin-like growth factors and neoplasia. Novartis Found Symp 2004;262:84–98 (discussion 98-107, 265-108).